ON THE NUMBER OF MODES IN SPHERICAL WAVE EXPANSIONS

Frank Jensen,
Aksel Frandsen

TICRA, Læderstræde 34, DK-1201 Copenhagen, Denmark

Abstract

Since the early days of spherical near-field far-field transformations a recommendation for the necessary number of polar modes has been given by $N = kr_o + 10$, k being the wavenumber and r_o the radius of the minimum sphere. The almost explosive development in computer speed and storage capacity witnessed during the last two decades has made transformations of fields from antennas exceeding thousands of wavelengths feasible, and a closer investigation of the above expression seems to be appropriate.

An improved expression for the number of modes, N, related to the antenna size and the required accuracy will be developed. The impact of truncation of the modal expansion at a given level will be illustrated. This is especially important for measurements where noise is present, or where there is undesirable scattering from objects.

Keywords: Noise Filtering, Number of Modes, Spherical Expansion, Spherical Modes, Spherical Near Field, Spherical Waves

1. Introduction

The field from an antenna may be expressed as a weighted sum of spherical modes. With a sufficient number of modal coefficients the field may be accurately calculated in all directions and at all distances greater than a mode-dependent minimum distance.

The number of modes depends on the variations of the field in θ and ϕ (spherical angles of the field direction in standard spherical coordinates). Field variations in ϕ are limited by the order M and field variations in θ are limited by the degree N. For the general case $M = N$ and the total number of modes is $2N(N+2)$. For antennas with some rotational symmetry around the z-axis we may have $M \ll N$.

An empirical value for N is

$$N = kr_o + n_1 \qquad (1)$$

where $k = 2\pi/\lambda$ is the wavenumber and r_o the radius of the minimum sphere, i.e. the smallest sphere centred at the origin and completely enclosing all radiating and scattering parts of the antenna.

In the early days of spherical near-field far-field transformations [1,2] computer limitations made it unrealistic to handle antennas with a diameter exceeding $\sim 100\lambda$. This led to $n_1 = 10$ in Eq. (1):

$$N = kr_o + 10 \qquad (2)$$

which has been widely adopted since then. Present day computers do not impose this restriction on antenna size, and antennas exceeding 1000λ in diameter may easily be treated. We therefore need to re-evaluate the estimate of n_1.

Turchin and Tseytlin [3] have stated that

$$n_1 = o(\sqrt[3]{kr_o}) \qquad (3)$$

but neither a justification nor a parametric expression have been presented.

2. The spherical waves

The electric field $\vec{E}$ radiated from a source of limited extent can be expressed as a weighted sum of spherical waves (Hansen [4]),

$$\vec{E}(r,\theta,\phi) = \frac{k}{\sqrt{\eta}} \sum_{s=1}^{2} \sum_{n=1}^{N} \sum_{m=-n}^{n} Q_{smn} \vec{F}_{smn}(r,\theta,\phi) \qquad (4)$$

at a field point (r,θ,ϕ). The field is fully characterised by the modal coefficients Q_{smn} to the spherical wave functions $\vec{F}_{smn}(r,\theta,\phi)$. The order m is limited by $|m| \le n$ and the degree n is limited by the extent of the sources given by N. The index s takes on the value 1 for TM fields and 2 for TE fields.

The spherical wave functions are power normalised such that the power of the radiated field given by Eq. (4) is

$$P_{rad} = \frac{1}{2} \sum_{smn} |Q_{smn}|^2 \quad \text{(watt).} \qquad (5)$$

Paper presented at AMTA 2004:
Published in Proc. 26th AMTA, Stone Mountain Park, GA, Oct. 17-22, pp. 489-94

This expression may be rewritten as

$$P_{rad} = \sum_{n=1}^{N} P_{rad}^{(n)} \tag{6}$$

where $P_{rad}^{(n)}$ is the power spectrum in n

$$P_{rad}^{(n)} = \frac{1}{2}\sum_{sm}|Q_{smn}|^2 \tag{7}$$

A similar power spectrum $P_{rad}^{(m)}$ may be defined in m.

For a truncation of the modes at $N_t < N$ it is of interest to know the amount of the truncated (i.e. excluded) power

$$P_{tr}^{(N_t)} = P_{rad} - \sum_{n=1}^{N_t} P_{rad}^{(n)} = \sum_{N_t+1}^{N} P_{rad}^{(n)} \tag{8}$$

Unless otherwise stated, the power content of the spectra presented here is normalised to $P_{rad} = 1$.

The r-dependence of the spherical wave functions is closely related to the spherical Hankel functions, $h_n(kr)$. At large distances r, $kr > n$, the Hankel functions represent a radiating field:

$$h_n(kr) \cong j^{n+1}\frac{e^{-jkr}}{kr} \tag{9}$$

while for small r, $kr < n$, it represents sources (the amplitude tends to infinity) cf. Figure 1, which shows the real and imaginary parts of the Hankel function $h_{30}(kr)$.

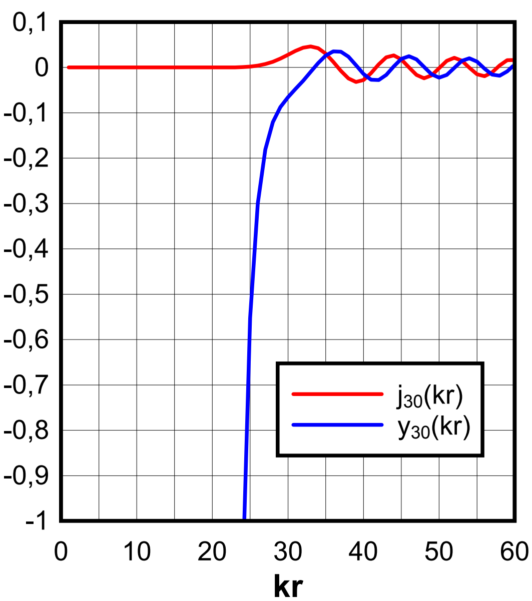

Figure 1 Real part (the Bessel function $j_{30}(kr)$) and imaginary part (the Neumann function $y_{30}(kr)$) of the Hankel function $h_{30}(kr)$, linear scale.

Correspondingly, Figure 2 shows how the Hankel functions for a fixed argument, $kr = 30$, are small when the order, n, is smaller than the argument, and increases drastically when the order exceeds the argument.

This is important for the expansion coefficients in Eq. (4). When the sources are bounded by a sphere of radius r_o, then the field is limited in amplitude outside this sphere, and all coefficients with $n > kr_o$ must vanish in order to balance out the values of the Hankel functions which increases so drastically with n. This is the physical background for the existence of an upper limit, $N \cong kr_o$, for the coefficients.

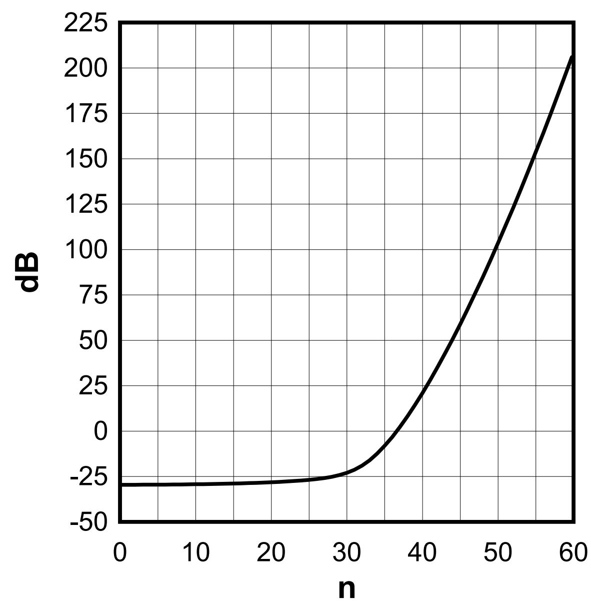

Figure 2 Amplitude of $h_n(30)$, $n = 0,1,\ldots,60$ in dB.

In order to obtain the required modal coefficients the field must be sampled with a spacing less than $180°/N$ in both θ and ϕ. When $M < N$ the sampling in ϕ may be increased to $180°/M$.

If the field is not reconstructed from the spherical modes but from interpolation in the sampled values then the spacing must be at least four times denser in θ as well as in ϕ.

3. Expansion of the field of a Hertzian dipole

A very simple field expansion is that of a $\hat{z}$-directed Hertzian dipole at the origin of the coordinate system. The field of this dipole is expressed by only one wave function $\vec{F}_{201}(r,\theta,\phi)$. As the Hertzian dipole is infinitesimally small we have $r_o = 0$ and $N = 1$.

3.1 The Hertzian dipole at $kr_o = 30$

If the Hertzian dipole is translated to the position $(x, y, z) = (r_o, 0, 0)$ with $r_o = 4.77\lambda$ ($kr_o = 30$) then the expansion involves at least the coefficients with $n \leq 30$.

The power spectrum for the translated dipole is shown in Figure 3 together with the truncated power, i.e. the power excluded when the mode series is truncated at the actual n, cf. Eqs. (7) and (8).

It is seen that the significant modes exist up to $n = kr_o$ but still a relative power about -15 dB is excluded if the mode series is truncated here. A more reasonable truncation is at $N = kr_o + 10 = 40$ where the excluded power is reduced to -70 dB.

Rotating the dipole to a different orientation will not change the power spectrum significantly.

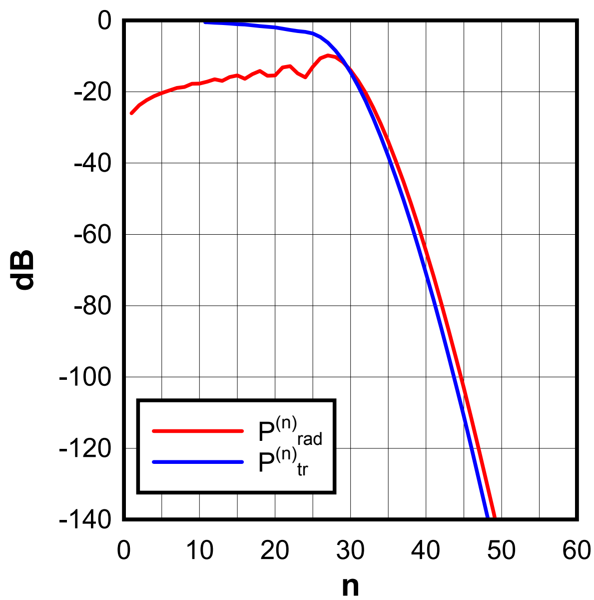

Figure 3 Power spectrum $P_{rad}^{(n)}$ and truncated power $P_{tr}^{(n)}$ for a $\hat{z}$-directed Hertzian dipole at $kr_o = 30$.

3.2 Truncating the mode series

When the mode spectrum is truncated at a given N, then the difference between the ideal field and the truncated field expresses an error field which in measurements shall be less than the field of the measurement noise.

It is characteristic for the truncated field – as well as for the error field – that it contains lobes with a lobe width of $180°/(N+1)$, cf. Figure 4, and that the level (here -60 dBi) is closely related to the truncation level in the mode spectrum (-70 dB at $N = 40$), cf. Figure 3.

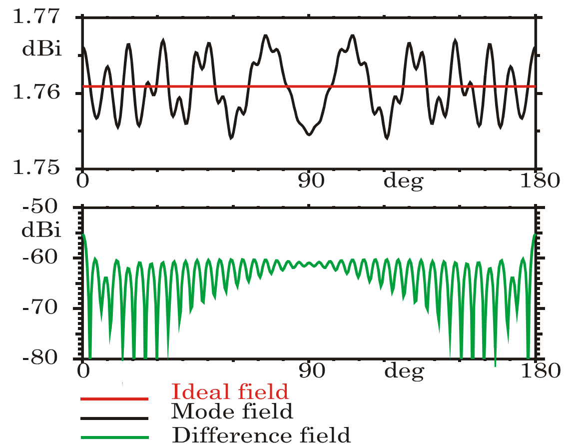

Figure 4 The far field for $\theta = 90°$ of the $\hat{z}$-directed dipole at $kr_o = 30$. Top: ideal field and field based on $N = 40$ modes. Bottom: difference field with 41 lobes.

In measurements, noise will cause the power spectra to reach a floor given by the noise level. The modes shall then be truncated when the noise level is reached. Truncation ripples as described above can only be avoided by multiplying the coefficients related to the noise by suitable weights decaying with n [5].

3.3 The Hertzian dipole at kr_o up to 3000

If we move the dipole further away from the centre of the expansion we get power spectra like that of Figure 3. In Figure 5 the spectra for $\hat{z}$-directed dipoles at $kr = 30$,

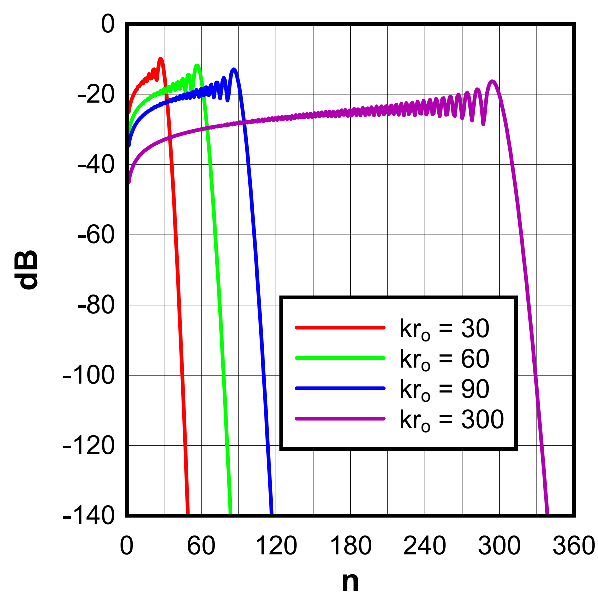

Figure 5 Power spectrum $P_{rad}^{(n)}$ for Hertzian dipoles at different positions r_o.

60, 90 and 300 are shown, and in Figure 6 the power spectrum for a $\hat{z}$-directed dipole at $kr = 3000$ is given.

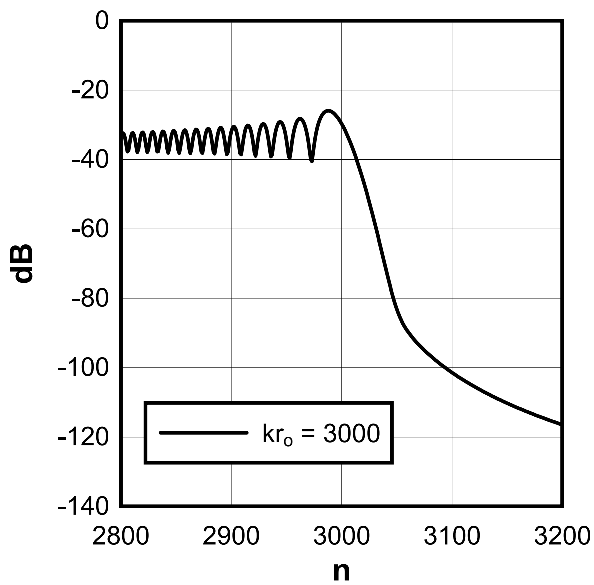

Figure 6 Part of the power spectrum $P_{rad}^{(n)}$ for a Hertzian dipole at $kr_o = 3000$.

It is seen that all spectra have a maximum near $n = kr_o$ and that the maximum decays for increasing n. This effect is simply due to the spectra being normalised to a total power of 1 and for increasing kr_o the power shall be distributed among an increasing number of modes.

The spectrum in Figure 6 does not fall steeply for levels below -80 dB because the modes in that case were calculated from field values which were truncated to 8 digits.

3.4 Scaled power spectra

As seen the spectra of Section 3.3 are similar. In fact by scaling the spectrum for a given kr_o in n to n',

$$n' - 300 = (n - kr_o)A \tag{10}$$

and by adding the power dP the spectrum will follow that of $kr_o = 300$ in the important fall-off region for $n > kr_o$, as shown in Figure 7.

The scaling factors A and dP have been determined for a set of kr_o-values by requiring the curves to coincide at -40 dB. The factors are seen to depend linearly on kr_o in double logarithmic scales, cf. Figure 8.

We may thus state that the power spectra drop, say 60 dB, from $n = kr_o$ by increasing n to $kr_o + n_1$ where

$$n_1 = 24 / A \cong 3.6 \sqrt[3]{kr_o} \tag{11}$$

applying Eq. (10) and A obtained from Figure 8:

$$10 \log A \cong -3.3 \log \frac{kr_o}{300} \quad \text{or} \quad A \cong \frac{6.7}{\sqrt[3]{kr_o}} \tag{12}$$

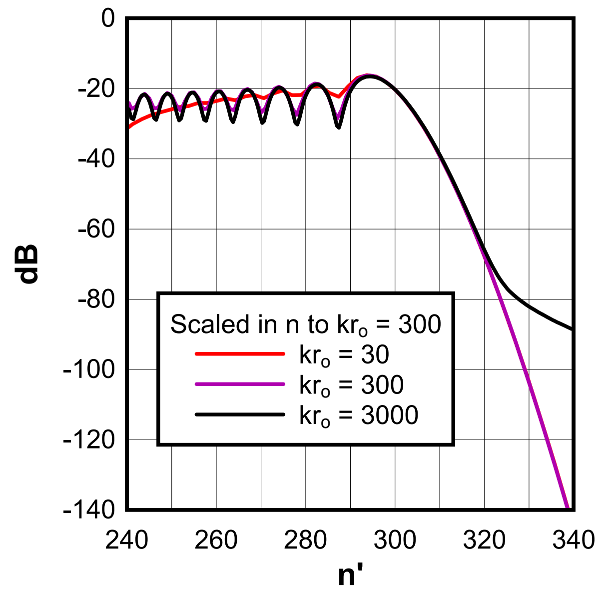

Figure 7 Part of the power spectra, scaled in n, for Hertzian dipoles at $kr_o = 30$, 300 and 3000. The last case is inaccurate below -70 dB.

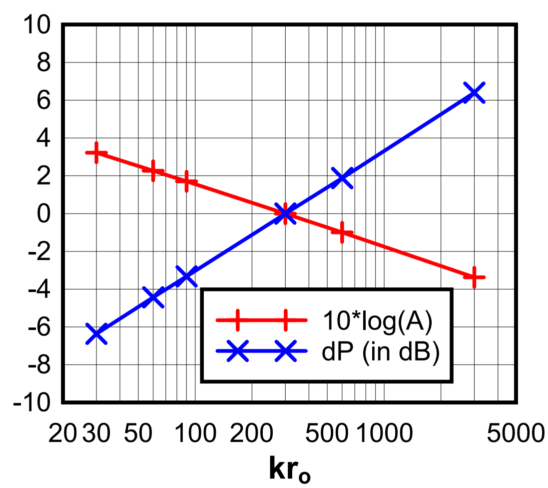

Figure 8 Scaling factors for the power spectra.

3.5 Number of modes versus truncated power

It is, however, not practical to evaluate the level of the spectrum at $n = kr_o$ and instead we will consider the amount of truncated power $P_{tr}^{(n)}$. Scaling of these functions in n turns out to give nearly identical curves, cf. Figure 9, though all curves are normalised to a total power of 0 dB (i.e. $dP = 0$). The curves accurately follow the curve for the scaled power spectra (thin line).

Thus, if we want to exclude no more than the power fraction P_{tr} (in dB) of a mode spectrum for an elementary source at the distance r_o from the centre of the expansion, then we must include $N = kr_o + n_1$ modes where n_1 may be read from Figure 9 and subsequently use Eq. (10):

P_{tr}	-40 dB	-60 dB	-80 dB	-120 dB
n_1	$1.6\sqrt[3]{kr_o}$	$2.5\sqrt[3]{kr_o}$	$3.6\sqrt[3]{kr_o}$	$5.0\sqrt[3]{kr_o}$

This may conveniently be approximated by (P_{r_o} and P_{tr} in dB)

$$N = kr_o + 0.045\sqrt[3]{kr_o}(P_{r_o} - P_{tr}) \tag{13}$$

in agreement with [3] and shown as the straight green line in Figure 9. P_{r_o} is the power of the source at $r = r_o$ relative to the total power. Here, in the dipole cases, $P_{r_o} = 0$ dB.

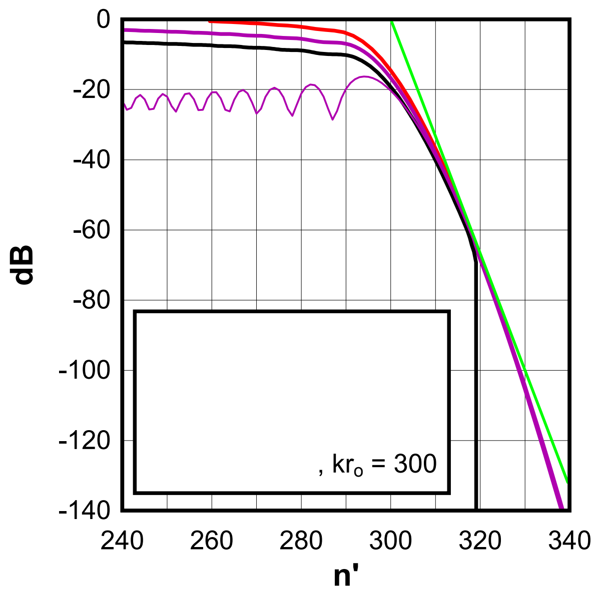

Figure 9 The truncated power $P_{tr}^{(n)}$ scaled in n, for Hertzian dipoles at $kr_o = 30$, 300 and 3000 and the power spectrum $P_{rad}^{(n)}$ for $kr_o = 300$.

3.6 Superposition

The spherical wave expansion is a linear transformation and superposition therefore valid. Consider three dipoles at $r = 4.77\lambda$ $(kr = 30)$, 9.54λ $(kr = 60)$ and 14.32λ $(kr = 90)$ excited by -0.31 dB, -10.31 dB and -20.31 dB, respectively (resulting in a total power 0 dB). The power spectrum, cf. Figure 10, is a weighted sum of the spectra of each dipole in Figure 5.

It is also seen how the truncated power for the two inner elements have vanished for $n \geq 90$. The truncated power for the three dipoles follows that of the outer element according to its excitation, $P_{r_o} = -20.31$ dB. Eq. (13) yields $N = 102$ in agreement with Figure 10.

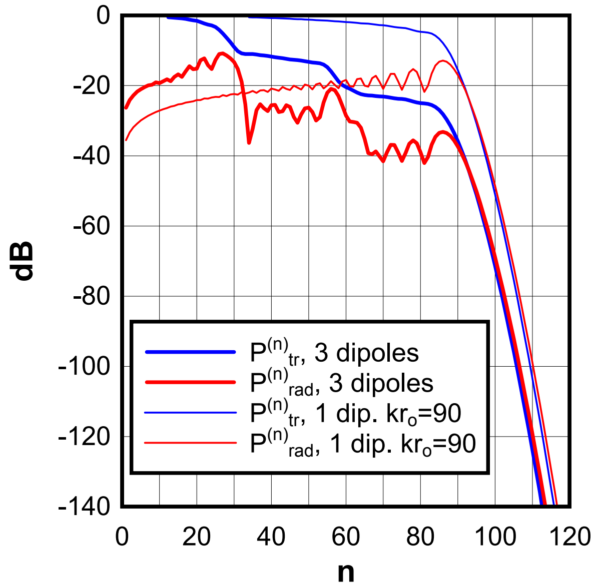

Figure 10 Truncated power $P_{tr}^{(n)}$ and power spectrum $P_{rad}^{(n)}$ for an array of three Hertzian dipoles compared to those for the outmost dipole alone.

4. Expanding the field of a reflector antenna

The principle of superposition may be applied in general. As an example we consider an offset reflector antenna of radius $r = 14.3\lambda$ ($kr = 90$), cf. Figure 11. The field is sampled on a sphere centred at the reflector centre, O.

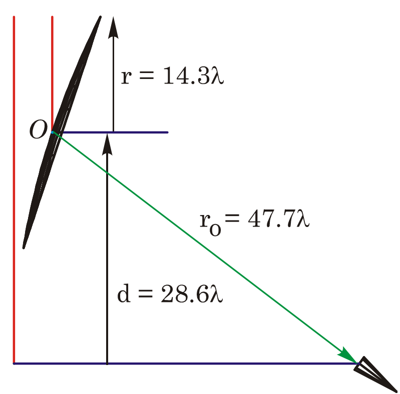

Figure 11 Off-set reflector antenna.

The field is calculated by physical optics (PO). First we compute the currents induced by the feed on the reflector surface. These currents in turn generate the scattered PO field, to which the feed field (black and blue patterns, respectively) must be added in order to give the total field (green pattern), cf. Figure 12.

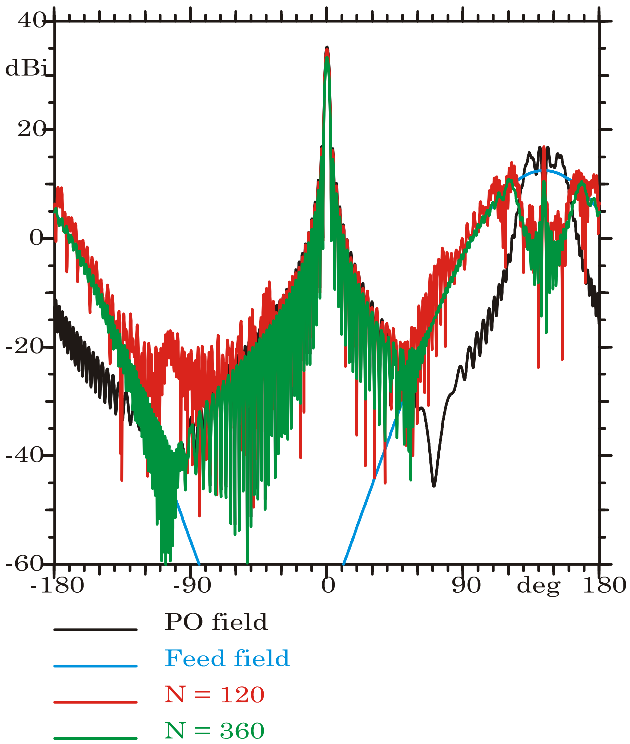

Figure 12 Patterns of the off-set reflector antenna.

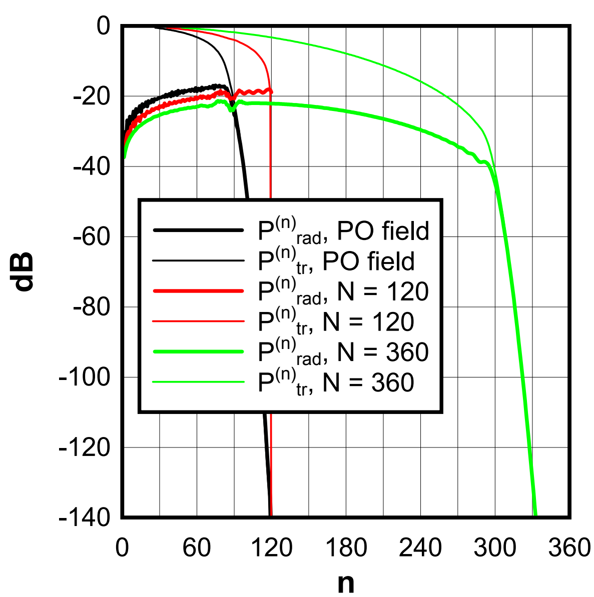

Figure 13 Mode spectra of the reflector antenna and of the reflector PO field alone.

The mode spectrum of the PO field is shown in Figure 13. Note that the mode power vanishes for $kr > 90$ as all PO-sources are inside this radius.

For the total field, however, the modes contain significant power at larger n and the pattern based on a mode set with $N = 120$ is insufficient to describe the far-out lobes (red curve in Figure 12). This is due to the feed being at $r_o = 47.7\lambda$ requiring $N > kr_o = 300$. The mode spectrum up to $N = 360$ is also shown in Figure 13 and the corresponding total field is shown in Figure 12 (green curve).

It is seen that it is important to include all sources (here the feed) when the radius of the minimum sphere is determined. This is of significant importance in measurements where scattering in the supporting structure may contribute to the measured field. An example of the influence of an absorber covering the back mounting of a low-gain antenna is given in [5].

5. Conclusion

An improved expression for the number of polar modes required for a spherical expansion of the field of sources located inside the minimum sphere of radius r_o has been derived. The expression is valid for all types of finite sources and determines the maximum spacing for sampling the field.

The impact of truncation of the modal expansion at a given level has been illustrated. This is particularly important for measurements where noise is present, or where there is undesirable scattering from objects.

6. References

[1] Jensen, F., "The influence of inaccuracies of measurements on antenna near-field – far-field correlation", *Proc. Fourth Coll. on Microwave Communication*, Budapest April 1970, Vol.III, paper ET-13.

[2] Jensen, F., "Electromagnetic near-field – far-field correlations", Ph.D. dissertation LD 15, Lab. of Electromagnetic Theory, Technical University of Denmark, 1970.

[3] Turchin, V.I., Tseytlin, N.M., "Antenna testing based on near-field measurements (Review)", *Radio Engineering and Electronic Physics*, Vol. 24, pp. 1-26, Dec. 1979.

[4] Hansen, J.E., "Spherical Near-Field Antenna Measurements", Peter Peregrinus Ltd., London, 1988.

[5] Lemanczyk, J. and Jensen, F., "The calibration of probes for near-field measurements", *AMTA-91*, Boulder, CO, pp 9-5 – 9-10, Oct. 1991.